



## Short communication

cDNA cloning and mRNA expression of four glutathione S-transferase (GST) genes from *Mytilus galloprovincialis*Chunyan Wang<sup>a,b</sup>, Jianmin Zhao<sup>b</sup>, Changkao Mu<sup>a,\*</sup>, Qing Wang<sup>b</sup>, Huifeng Wu<sup>b</sup>, Chunlin Wang<sup>a,\*</sup><sup>a</sup> School of Marine Science of Ningbo University, 818 of Fenghua Rd., Ningbo 315211, PR China<sup>b</sup> Key Laboratory of Coastal Zone Environment Processes, CAS, Shandong Provincial Key Laboratory of Coastal Zone Environment Processes, Yantai Institute of Coastal Zone Research, Chinese Academy of Sciences, Yantai 264003, PR China

## ARTICLE INFO

## Article history:

Received 4 September 2012

Received in revised form

3 November 2012

Accepted 11 November 2012

Available online 14 December 2012

## Keywords:

*Mytilus galloprovincialis*

Molecular cloning

Glutathione S-transferases

Innate immune

## ABSTRACT

Glutathione S-transferases (GSTs) are phase II enzymes involved in the regulation of redox homeostasis and innate immune responses against bacterial infection, which also play important roles in the detoxification of xenobiotics. In this study, we reported four genes of the GST family (named MgGST $\alpha$ , MgGSTS1, MgGSTS2, and MgGSTS3, respectively) from *Mytilus galloprovincialis*. MgGST $\alpha$ , MgGSTS1, MgGSTS2, and MgGSTS3 consisted of open reading frame (ORF) of 648 bp, 612 bp, 621 bp and 609 bp respectively, which encoded proteins of 216, 204, 207 and 203 amino acids residues, respectively. Sequence analysis showed that the predicted protein sequence of MgGSTs contained the conserved domain of the GST\_N and GST\_C. Alignment analysis indicated that the MgGSTs were divided into two types, one was of alpha GST, and the others were of sigma class. Tissue distribution study revealed that MgGST $\alpha$ , MgGSTS2, MgGSTS3 transcripts were highly expressed in hemocytes, while MgGSTS1 mRNA was most abundantly expressed in hepatopancreas. After bacterial challenge, the expression level of these MgGSTs in hemocytes were all significantly higher than that of the control group. These results suggested that MgGSTs might play important roles in the modulation of immune response in *M. galloprovincialis*.

© 2012 Published by Elsevier Ltd.

## 1. Introduction

In marine environments, bivalves are commercially and ecologically important as food and non-food resources. Because of their benthic and sedentary mode of life, they are easily exposed to biotic and abiotic stresses, such as various pathogens and pollutants [1]. Reactive oxygen species (ROS) such as hydrogen peroxide (H<sub>2</sub>O<sub>2</sub>) and superoxide anion (O<sub>2</sub><sup>-</sup>) are usually generated in response to these stresses [2,3]. Organisms have evolved different strategies to cope with the negative physiological effects of ROS by a group of antioxidant enzymes, such as superoxide dismutase (SOD), catalase (CAT), glutathione peroxidase (GPx), glutathione-S-transferase (GST) and some non-enzymatic antioxidant molecules [1,4].

Among the antioxidant enzymes, glutathione S-transferase (GST, EC 2.5.1.18) is a multifunctional dimeric protein involved in cellular detoxification of reactive electrophilic compounds, and protecting tissues against oxidative damage [5,6]. Currently, at least 15

different classes of GSTs (alpha, beta, delta, epsilon, kappa, lambda, mu, omega, phi, pi, sigma, tau, theta, zeta, and rho) have been reported in numerous organisms based upon their substrate specificity, antibody cross-reactivity and sensitivity to inhibitors [5,7].

*Mytilus galloprovincialis* is widely distributed around the coastal area, and is susceptible to suffering serious problems such as bacterial infection and pollution exposure [8]. However, most mussels could survive in this environment owing to their strong immune system and detoxification ability [9]. So, it is interesting to investigate the resistance mechanisms of mussels to pathogenic infection and oxidative damage. In this study, four GSTs genes from *M. galloprovincialis* were identified and characterized. To further characterize the roles of MgGSTs in innate immune responses, the expression patterns of these four MgGSTs were also investigated after the mussels were challenged with *Listonella anguillarum*.

## 2. Materials and methods

2.1. Animal culture and *L. anguillarum* challenge

Adult mussels *M. galloprovincialis* about 4 cm in shell length were purchased from a local farm and acclimatized for 10 days

\* Corresponding authors. Tel.: +86 574 87600356; fax: +86 574 87608347.

E-mail addresses: [muchangkao@nbu.edu.cn](mailto:muchangkao@nbu.edu.cn) (C. Mu), [wangchunlin@nbu.edu.cn](mailto:wangchunlin@nbu.edu.cn) (C. Wang).

at 18–20 °C. After acclimation, the mussels were divided into six 50L-tanks, each containing 50 individuals. During the whole experiment, mussels were fed with *Isochrysis galbana* and *Platymonas helgolandica*, with sea water (32 psu) totally changed daily.

The mussels were injected into adductor muscle with 50 µL of live *L. anguillarum* (final concentration of  $10^7$  CFU mL<sup>-1</sup>) suspended in phosphate buffered saline (PBS, pH 7.4) or the same volume of PBS (control group). For *L. anguillarum* challenge experiment, one tank was served as control. The other six injected mussels were randomly sampled at 12 h, 24 h, 48 h and 96 h after bacterial challenge. The hemolymph was collected from the adductor muscle using a syringe and centrifuged (2000 g for 10 min at 4 °C) to harvest the hemocytes. The gills, adductor muscle, mantle, gonad, hemocytes and hepatopancreas from the control were sampled to determine the tissue distribution of MgGST $\alpha$ , MgGSTS1, MgGSTS2, MgGSTS3 transcripts, and hemocytes from the control and infected groups were sampled to determine the expression levels of MgGST $\alpha$ , MgGSTS1, MgGSTS2, MgGSTS3 transcripts after bacteria stimulation.

## 2.2. Cloning the full-length cDNAs of MgGSTs

Total RNA from different tissues was extracted by using Trizol Reagent (Invitrogen, USA). One microgram of total RNA was subjected to cDNA synthesis with M-MLV reverse transcriptase (Promega) as previously described [10]. The 3' ends of MgGSTs was obtained by rapid amplification of cDNA ends (RACE) using the 3'-Full RECA Core Set Ver.2.0 (20 RT Reactions) Kit (TaKaRa, Japan) according to manufacturer's recommendations. The primers used for cloning the full-length cDNAs of MgGSTs were listed in Table 1. The resultant PCR products were cloned into pMD18-T vector (Takara, Japan), and then transformed into *Escherichia coli* Top10F' competent cells. For sequence confirmation, three positive clones

for each MgGST were sequenced on an ABI3730 Automated Sequencer (Applied Biosystem, USA).

## 2.3. Sequence analysis

The cDNA and amino acid sequences of MgGSTs were analyzed using the BLAST program (<http://www.ncbi.nlm.nih.gov/blast>) and the Expert Protein Analysis System (<http://www.expasy.org/>). The "GST\_N\_alpha-like", "GST\_C\_alpha-like", "GST\_N\_sigma-like" and "GST\_C\_sigma-like" were predicted using the CD-Search in NCBI's CDD (<http://www.ncbi.nlm.nih.gov/Structure/cdd/wrpsb.cgi>). Multiple alignments were performed with the ClustalW multiple alignment program (<http://www.ebi.ac.uk/clustalw>) and multiple alignment show program (<http://www.biosoft.net/sms/index.html>). A phylogenic NJ tree was constructed with the neighbor-joining (NJ) method embedded in Mega 4 software package [11]. To derive the confidence value for the phylogeny analysis, bootstrap trials were replicated 1000 times.

## 2.4. Tissue distribution and temporal expression of MgGSTs mRNA in hemocytes after *L. anguillarum* challenge

Tissue distribution of MgGSTs and their responses to *L. anguillarum* challenge were measured by QRT-PCR in Applied Biosystem 7500 System. The primers used for real-time RT-PCR were listed in Table 1. Each assay was performed in triplicate with  $\beta$ -actin mRNA as the internal control. The reaction component and thermal profile were conducted as previously described [10]. All data were presented as means  $\pm$  S.E., and subjected to one-way analysis of variance (one-way ANOVA). In all cases, *P*-value less than 0.05 were considered statistically significant.

## 3. Results

### 3.1. Sequence and phylogenetic analysis

Four nucleotide sequences of 842 bp, 1047 bp, 729 bp and 785 bp representing the complete cDNA sequence of MgGST $\alpha$  (Fig. 1A), MgGSTS1 (Fig. 1B), MgGSTS2 (Fig. 1C), and MgGSTS3 (Fig. 1D), respectively, were obtained by overlapping EST with the fragments amplified by RACE. The deduced amino acid sequences of MgGST $\alpha$ , MgGSTS1, MgGSTS2, and MgGSTS3 were shown in the corresponding nucleotide acid sequence in Fig. 1. Based on the deduced amino acid identities and phylogenetic analysis with other GSTs, the four MgGSTs were categorized into two classes, sigma type (MgGSTS1, MgGSTS2 and MgGSTS3, GenBank accession number JX485636, JX485637, JX485738, respectively) and alpha type (MgGST $\alpha$ , GenBank accession number JX485635). Among these GSTs, MgGST $\alpha$  had the highest molecular weight (24.9 kDa) and MgGSTS3 possessed the lowest molecular weight (22.8 kDa), MgGSTS2 and MgGSTS3 contained a molecular mass 23.6 kDa and 23.3 kDa respectively. The putative MgGST $\alpha$ , MgGSTS1, MgGSTS2 and MgGSTS3 proteins were calculated to have a theoretical pI of 5.48, 5.26, 8.88 and 5.44. SMART analysis revealed that the predicted protein sequence of MgGST $\alpha$  contained the conserved domain of GST\_N\_alpha-like (from Tyr<sup>3</sup> to Arg<sup>75</sup>) and GST\_C\_alpha-like (from Ile<sup>69</sup> to Asp<sup>188</sup>). Similarly, the GST\_N\_sigma-like and GST\_C\_sigma-like domains were also identified in the three sigma type MgGSTs, respectively. A consensus polyadenylation site (AATAAA) were located downstream of the translation termination codon in MgGST $\alpha$ , MgGSTS1 and MgGSTS2.

The deduced amino acid sequences of MgGSTs showed high similarities to counterparts of other species (Fig. 2). For example, three sigma type GST identified from *M. galloprovincialis* shared high similarity with sigma GST from *Haliotis discus discus*

**Table 1**  
Oligonucleotide primers used in the experiment.

Primer Sequence(5'–3')	Sequence information
P1(forward)	GTAGACATGTACTATGAAGGATC MgGST $\alpha$ specific outer primer
P2(forward)	GGACTGCTTGACTGCCTGTT MgGST $\alpha$ specific inner primer
P3(forward)	GATTCTGTGCGATTGGAG MgGSTS1 specific outer primer
P4(forward)	ACTAACAGCAAGAAAGGCG MgGSTS1 specific inner primer
P5(forward)	GCGATGAAGAAATTAATGAAG MgGSTS2 specific outer primer
P6(forward)	ATGTATTGGAAGGTGCTGTC MgGSTS2 specific inner primer
P7(forward)	AACITTTAAAGGAGAATTCTCTAC MgGSTS3 specific outer primer
P8(forward)	TAATGACTACTCCGCGATAC MgGSTS3 specific inner primer
P9(reverse)	TACCGTCGTTCCACTAGTGATTT 3'RACE Outer Primer
P10(reverse)	CGCGGATCTCCACTAGTGATTT 3'RACE Inner Primer
P11(forward)	GCTATCCAGGCCGTACTCT Real time $\beta$ -actin primer
P12(reverse)	GCGGTGGTTGTGAATGAG Real time $\beta$ -actin primer
P13(forward)	ATCAGGAGGCTGCCAAAGTA Real time MgGST $\alpha$ primer
P14(reverse)	CTACAGCCAACAGGCACTCA Real time MgGST $\alpha$ primer
P15(forward)	GGAGCTGGCTCGTATCATGT Real time MgGSTS1 primer
P16(reverse)	TGCAATGGCCATAGACTGAG Real time MgGSTS1 primer
P17(forward)	TGAAGCAAGAAAGGCAGAGG Real time MgGSTS2 primer
P18(reverse)	CAAGCCTTTACATCCGGGTA Real time MgGSTS2 primer
P19(forward)	AAGGAAAGCAAGGGGTGAA Real time MgGSTS3 primer
P20(reverse)	GAAATGGCACCACTCTGGTT Real time MgGSTS3 primer

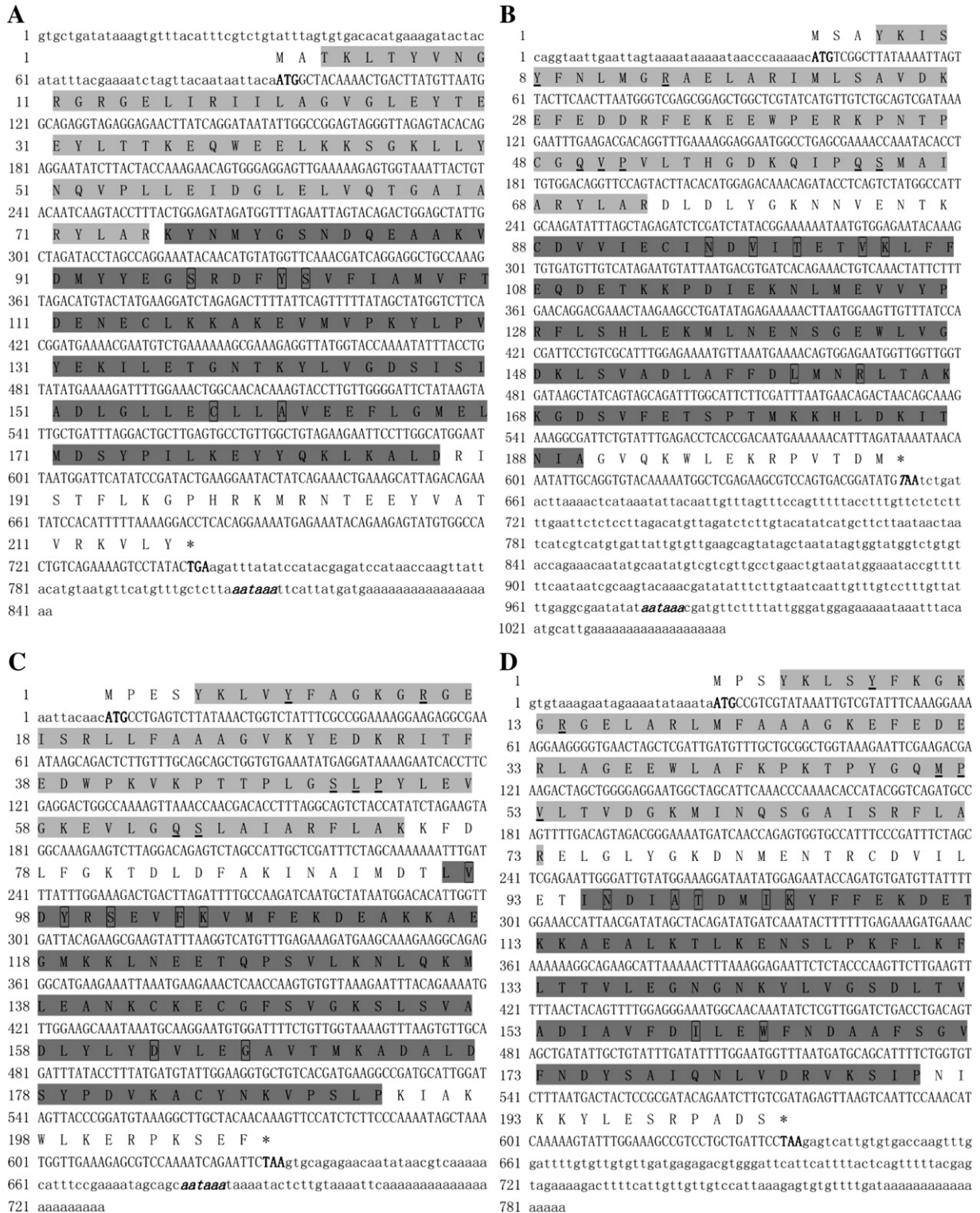


**Fig. 1.** Nucleotide and deduced amino acid sequences of MgGST $\alpha$  (A), MgGSTS1 (B), MgGSTS2 (C), and MgGSTS3 (D). The start and stop codons are marked in bold. The classical polyadenylation signal in the 3'-UTR is in bold and italicized. The conserved domains GST\_N is shaded in gray. The predicted conserved domains GST\_C is shaded in dark. GSH-binding sites (G-site) in N-terminal is underlined. Sites of substrate binding pocket (H-site) in C-terminal is boxed.

(ABO26603.1), *Chlamys farreri* (ACF25904.1), *Branchiostoma floridae* (XP\_002605352.1), *Ruditapes philippinarum* (AEW46326.1) and *Haliotis diversicolor* (ABV01122.2), while MgGST $\alpha$  shared high identity of 48% with *H. discus discus* GST $\alpha$  (ABO26598.1), 45% identity with *B. floridae* GST $\alpha$  (XP\_002590293.1) and 44% with *Perinereis nuntia* GST $\alpha$  (AEI70672.1).

To evaluate the molecular evolutionary relationships of GSTs, we constructed an un-rooted phylogenetic tree using the NJ method. According to the phylogenetic tree (Fig. 3), MgGSTS1, MgGSTS3 and MgGSTS2 clustered with the mollusc sigma type GSTs, while MgGST $\alpha$  formed its own clades with alpha type GSTs from other organisms.

MgGSTalpha	M A T K - - L T Y V N G R G R C E T I R I I L A G V G L E Y T E E Y L T T K E Q	38
Haliotis_discus_discus	M A S E P H L T Y F E G R G F G E L T R M T L C A A R I K F T E H F V Q S R E E	40
Perinereis_nuntia	- - - - V K L H Y F N G R G L G E R V R L M L C L A G V K F E E V L L T E R S Q	36
ranchiostoma_floridae	M S Q K A R L T Y F N G R G R C E S T R F M L G A A G F E F D E V F L E T K E Q	40
Ictalurus_punctatus	M S G K V V L Y Y F N G R G K M E S T R W L L A V A G V E F E E V H L T T K E Q	40
MgGSTalpha	W E E L K K S G K L L Y N Q V F L L E I D G L E L V Q T G A I A R Y L A R K K Y N	78
Haliotis_discus_discus	F L Q M K A D G K L L F G Q L P L L E I D G L K L I O R R A I L K Y L A R R E G	80
Perinereis_nuntia	M E K L I K D G D L L F G Q L P L L E I D G M K L V Q A N V C A R Y V A S R S N	76
ranchiostoma_floridae	M E E L R A R G D L L F L Q V P L L E I D G M K M V Q T G A M L R Y I A R K A S	80
Ictalurus_punctatus	F K K L V D D G A L L E R Q V P L V E M D G M K L V Q T K A I L N Y I A G K Y N	80
MgGSTalpha	M Y G S N D Q E A A K V D M Y Y E G S R D F Y S V F I A M V F T - - - D E N E C	115
Haliotis_discus_discus	L Y G S N P T E N A F V D M Y F E G T R D F M N A F D F W V F D - - - D V N K I	117
Perinereis_nuntia	M Y S T D P K V Q A R I D M L Y D G T R D F L M L F L L A G I K - - L S E E D L	114
ranchiostoma_floridae	L F G R D D K E S A R I D M L A D G V R D F Q L K F L G I P F Q - - S D P T E L	118
Ictalurus_punctatus	L Y G K D I K E R L M I D M Y S E G A R D I M D M I M I L P F T P A D Q K Q S Q	120
MgGSTalpha	L K K A K E V M V P K Y L F V Y E R I L E T G N T K Y L V G D S I S I A D L G L	155
Haliotis_discus_discus	R E A Y R T K H F P R Y L F V F E R V L Q E S S S G Y L V G E A M S L A D L A L	157
Perinereis_nuntia	K K K A T E K D F P R Y L F V F E K A L K E N G T G Y L V G N R P T L A D A G L	154
ranchiostoma_floridae	L A M I R D K D L P R Y L F Y D H V L Q D N G T G F L V G S L S M A D V L L	158
Ictalurus_punctatus	L D K I Q G K A K E R T L F A Y E K A L A H S - - Q Y L V G T Q L S C A D V H L	158
MgGSTalpha	L E C L L A V E E F L G M E L M D S Y P I L K E Y Y Q K L K A L D R I S T F L K	195
Haliotis_discus_discus	L E P L M T A H E C F G G R C S A G - - - - - L S Q I K G I P - - - - -	183
Perinereis_nuntia	L E D L L A L G D Y F G Q E P L K D Y P N L T V F L K K M K S L D G I K L Y L E	194
ranchiostoma_floridae	F E A L L S V D E V F - P E L L K D Y P K L Q E F R D R V A A Q P N M A K F L A	197
Ictalurus_punctatus	L E V T L M L E E V L - P T I L S T F P K I Q E F Q K R M K A I P A I S K F L Q	197
MgGSTalpha	G P - H R K M R N T E E Y V A T V R K V L Y - - - - -	216
Haliotis_discus_discus	- - - - - Q N D D N K - - - - -	189
Perinereis_nuntia	K Y - - R K R M N D A R Y K E E I V R V L G L T D S D L	220
ranchiostoma_floridae	G G - Q R K P P G D A V Y R N T V D T V L G R K - - -	220
Ictalurus_punctatus	P G S Q R K S P P D E V Y V K T V M N V L S H L F K - -	223
MgGSTS1	M S - - - - A Y K I S Y F N L M G R A E L A R I M L S A V D K E F E D D R F E	35
MgGSTS2	M P - - - - E S Y K L V Y F A G K G R G E I S R L L F A A A G V K Y E D K R I T	36
MgGSTS3	M P - - - - S Y K L S Y F K G K G R G E L A R L M F A A A G K E F E D E R L A	35
Solen_grandis	M A D K S K H S Y K L L Y F Q S R G V A E L I R L L F K V A E V D F E D K R Y S	40
Chlamys_farreri	M P - - - - T Y T L H Y F P L R A R G E L I R L L F A A A G K T Y T D K I I T	35
MgGSTS1	K E E W P E R K P N T P C G Q V P V L T H G D K Q I P Q S M A I A R Y L A R D L	75
MgGSTS2	F E D W P K V K P T T P L G S L P Y L E V G K E V L G Q S L A I A R F L A K K F	76
MgGSTS3	G E W L A F K P K T P Y G Q M P V L T V D G K M I N Q S G A I S R F L A R E L	75
Solen_grandis	R E E W P S Q K E A Q P L K A L P V L E V D G K K Y C L S A I A R Y L A E E F	80
Chlamys_farreri	F A D W P S K K S E M P T G Q L P V L E V D G E K I S Q S L A I S R Y L S R E F	75
MgGSTS1	D L Y G K N N V E N T K C D V V I E C I N D V I T E T V K L F F E Q D E T K K P	115
MgGSTS2	D L F G K T D L D F A K I N A I M D T L V D Y R S E V F K V M F E K D E A K K A	116
MgGSTS3	G L Y G K D N M E N T R C D V I L E T I N D I A T D M I K Y F F E K D E T K K A	115
Solen_grandis	G L M G S C P L D V L R I N E I Q E A V T E M F K D F F E I F Y E K D K D K K V	120
Chlamys_farreri	G L A G D S S L D Q A R T D Q V V D T I G D L L T E F F K Y A F E K D T E K K E	115
MgGSTS1	D I E K N L M E V V Y P R F L S H L E K M I N E N - S G E - - W L V G D K I S V	152
MgGSTS2	E G M K K L N E E T Q P S V L K N L Q K M E A N K C K E C G F S V G K S L S V	156
MgGSTS3	E A L K T L K E N S L P K F L K F L T T V L E G H - G N K - - Y L V G S D L T V	152
Solen_grandis	T M L Q K T N K E T L P K F L D F Y E K R L K E N N K G E - G W V V G D K L T L	159
Chlamys_farreri	E L K K K T F D S V L T T F A T N I T K F L D M N K D K S - G Y F V G K K L T A	154
MgGSTS1	A D L A F F D L M N R L T A K K G D S - - - V F E T S P T M K K H L D K I T N I	189
MgGSTS2	A D L Y L Y D V L E G A V T M K A D A - - - - L D S Y P D V K A C Y N K V P S L	192
MgGSTS3	A D I A V F D I L E W F N D A A F S G - - - V F N D Y S A I Q N L V D R V K S I	189
Solen_grandis	A D L V L Y N T F H T I T L F M S M A G L N A L E K R P L L Q A H Y A R V E A L	199
Chlamys_farreri	A D L A V Y E G F E D F V L V D P K A - - - - L D K Y P K L V A H R K L V L S N	190
MgGSTS1	A G V Q K W L E K R P V T D M	204
MgGSTS2	P K I A K W L K E R P K S E F	207
MgGSTS3	P N I K K Y L E S R P A D S -	203
Solen_grandis	P Q I A A W I K A R P E T E N	214
Chlamys_farreri	P K V K A Y V D K R P K T D V	205

**Fig. 2.** Multiple alignment of MgCST $\alpha$ (A) and MgGSTS(B) with corresponding counterparts deposited in GenBank. The black shadow region indicates positions where all sequences share the same amino acid residue. Gaps are indicated by dashes to improve the alignment. The species and the GenBank accession no. are as follows: *Haliotis discus discus* (ABO26598.1), *Ictalurus punctatus* (NP\_001187537.1), *Perinereis nuntia* (AEI70672.1), *Branchiostoma floridae* (XP\_002590293.1), *Solen grandis* (AEW43451.1), *Chlamys farreri* (ACF25904.1).

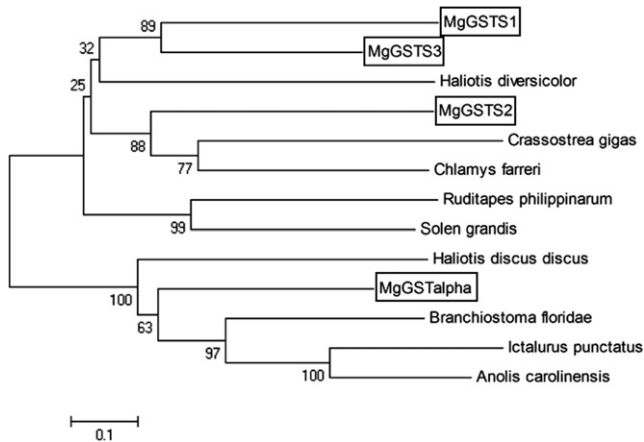


**Fig. 3.** Phylogenetic tree constructed by neighbor-joining method based on the sequences of GSTs from different animals. The numbers at the forks indicate the bootstrap values. The sequences were as follows: GST-alpha: *Haliotis discus discus* (ABO26598.1), *Ictalurus punctatus* (NP\_001187537.1), *Anolis carolinensis* (XP\_003215482.1), *Branchiostoma floridae* (XP\_002590293.1); GST-Sigma: *Solen grandis* (AEW43451.1), *Chlamys farreri* (ACF25904.1), *Ruditapes philippinarum* (ADI44317.1), *Haliotis diversicolor* (ABV01122.2), *Crassostrea gigas* (CAE11863.1).

### 3.2. Tissue distribution of MgGSTs mRNA

The tissue-specific expression of MgGSTs transcripts was determined by quantitative RT-PCR. It was found that MgGSTs mRNA was expressed in all tissues examined. As shown in Fig. 4, the highest expression level of MgGST $\alpha$ , MgGSTS2 and MgGSTS3 mRNA was detected in hemocytes. However, MgGSTS2 transcript was found to be most abundantly expressed in the tissue of hepatopancreas, and trace transcript was detected in the mantle and gills.

### 3.3. Temporal expression patterns of MgGSTs mRNA in hemocytes after bacterial challenge

QRT-PCR was employed to quantify the MgGSTs expression profiles after bacterial challenge with  $\beta$ -actin as internal control. For MgGSTs and  $\beta$ -actin genes, only one peak at the corresponding melting temperature was observed in the dissociation curve analysis, indicating that the PCR was specifically amplified (data not shown). During the whole experimental period, no notable change ( $P > 0.05$ ) of MgGSTs mRNA expression was observed for the control treatment. As shown in Fig. 5, the effect of *L. anguillarum* on *M. galloprovincialis* innate immunity was detected as soon as 12 h after exposure. The expression level of MgGSTS1, MgGSTS2, MgGSTS3 and MgGST $\alpha$  in hemocytes were all significantly up-regulated at different time intervals post bacterial challenge. Significant increase of MgGST $\alpha$  and MgGSTS3 expression level (3.5-fold and 4.2-fold higher than that of the control,  $P < 0.05$ , respectively) were detected at 48 h post infection, while the maximum expression level of MgGSTS1 and MgGSTS2 were detected at 12 h and 24 h after infection (5.2-fold and 36.1-fold compared with the control,  $P < 0.05$ , respectively). As time progressed, the expression of MgGSTS1, MgGSTS3 and MgGST $\alpha$  mRNA nearly returned to the baseline level at 96 h post-challenge (compared with the control,  $P > 0.05$ , respectively). At 12 h post-challenge, the expression level of MgGSTS2 mRNA was higher than that of the others (MgGST $\alpha$ , MgGSTS1, and MgGSTS3).

## 4. Discussion

Glutathione S-transferases are well-characterized family of multifunctional isoenzymes that are ubiquitously distributed in

bacteria, plants, and animals [12]. GSTs are a family of proteins which play important roles in the oxidative stress responses and the detoxification pathways [13]. Blast analysis revealed that MgGSTs shared relatively high homology with those from other organisms. The GST classes relied on their G-site homology and mechanisms and H-site homology [12]. Using the CD-Search in NCBI's CDD, the predicted protein sequence of MgGST $\alpha$  cDNA was matched to the GST\_N\_alpha\_like and GST\_C\_alpha\_like, containing an H-site which is a substrate binding site in the C-terminal [14]. The longer alpha C-terminal also forms an  $\alpha$ -helix, which is thought to be important to dimer stabilization and affects both the GSH-binding rate and the ionization state of the catalytically essential residue Tyr [15,16]. The sigma class GSTs are lacking in both components of the ball-and-socket interface, and rely on a Tyr residue for GSH stabilization in the G-site [12], which was also found in the sequence of MgGSTS1, MgGSTS2 and MgGSTS3. The G-site (responsible for tripeptide GSH binding) and H-site (accounting for the binding of xenobiotic compounds) are highly conserved in the four MgGSTs, respectively. So the four MgGSTs were categorized into two classes, sigma type (MgGSTS1, MgGSTS2 and MgGSTS3) and alpha type (MgGST $\alpha$ ). On the basis of all these typical description, MgGST $\alpha$ , MgGSTS1, MgGSTS2 and MgGSTS3 were proposed to be new members of the GSTs family.

As compared to vertebrate GSTs, there is a few information about the expression pattern of different classes of GSTs in mollusks so far. Ren et al. [14] reported that a high level of abGSTsigma transcripts was shown in the gill of *H. diversicolor*. Zhang et al. [7] suggested that the differences in tissue distribution of various GST isoforms were associated with differential susceptibility to antioxidant damage. In the present study, tissue distribution of MgGSTs revealed that they were generally abundantly expressed in hemocytes and hepatopancreas. Studies also showed that MgGST $\alpha$ , MgGSTS2 and MgGSTS3 transcripts were dominantly expressed in hemocytes, whereas MgGSTS1 exhibited the highest expression level in the tissue of hepatopancreas, and trace transcript of MgGSTS2 was detected in the gills and mantle. Members of the GST super family exhibit different primary structures, enzyme properties, and physiological functions [17]. These results suggested that each of the GST classes might have different distributions in tissues, and perhaps involved in some physiological functions in the basal metabolism of *M. galloprovincialis*.

Molluscs rely highly on their innate immunity, and hemocyte-mediated phagocytosis is one of the main arms of their innate-defense strategies [2]. The killing of pathogens by hemocytes is usually accompanied by a sudden release of ROS through the respiratory burst to clear the invading microorganism [18,19]. However, the homeostasis of redox balance in cells would be disrupted because of ROS generation. In the present study, the abundance of MgGSTs mRNA were up-regulated in the mass and increased significantly at different intervals due to the synergistic interaction of the oxidative system and anti-oxidative system for killing pathogens. It was suggested that the oxidative system was perhaps initially activated to maintain the high local concentration of ROS necessary for killing pathogens. Similar results were also reported in disk abalone (*H. discus discus*) and shrimp *Litopenaeus vannamei* [14,20,21]. As time progressed, the decrease of MgGSTs mRNA abundance was observed, perhaps because the anti-oxidative system was activated to clear excessive ROS after elimination of the pathogens. Notably, the expression level of MgGSTS2 mRNA was significantly higher than that of the other three MgGSTs at 24 h, 48 h and 96 h post bacterial challenge. It had been suggested that low constitutively expressed GST perhaps performed a crucial role in the detoxification process, whereas high induced expressed GSTs might involve in protecting the cell against endogenous oxidative stress [22–24]. These results suggested that

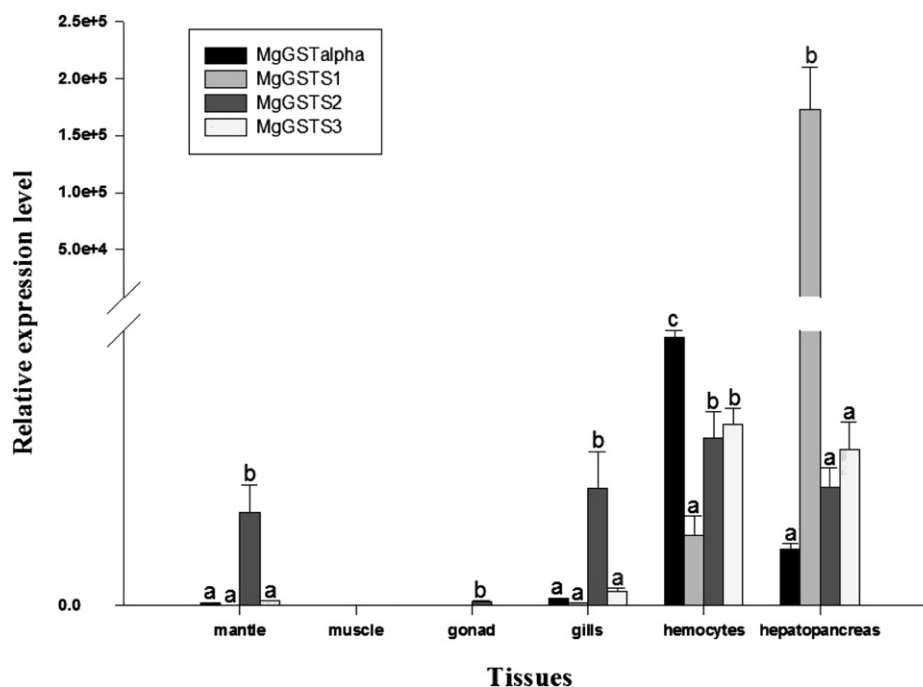


**Fig. 4.** MgGST $\alpha$ , MgGSTS1, MgGSTS2, and MgGSTS3 mRNA expression level in different tissues of adult clams detected by real-time PCR. The transcript level MgGSTs in hemocytes, gills, mantles, muscle, gonad, and hepatopancreas is normalized to that of adductor muscles, respectively. The results are shown as mean  $\pm$  S.E. ( $n = 4$ ), and bars with different letters are significantly different ( $P < 0.05$ ).

MgGSTS2 might play a leading role in immunization against pathogen infection, and the four MgGSTs isoforms exerted their function in a manner of synergy.

In conclusion, the full-length cDNA encoding four genes of the GST family (MgGST $\alpha$ , MgGSTS1, MgGSTS2, and MgGSTS3) were

isolated from *M. galloprovincialis*. All MgGSTs mRNA were constitutively expressed in the tested tissues, and were significantly up-regulated in hemocytes after bacterial challenge. These results suggested the involvement of MgGSTs in the defense response of *M. galloprovincialis* against bacterial infections.

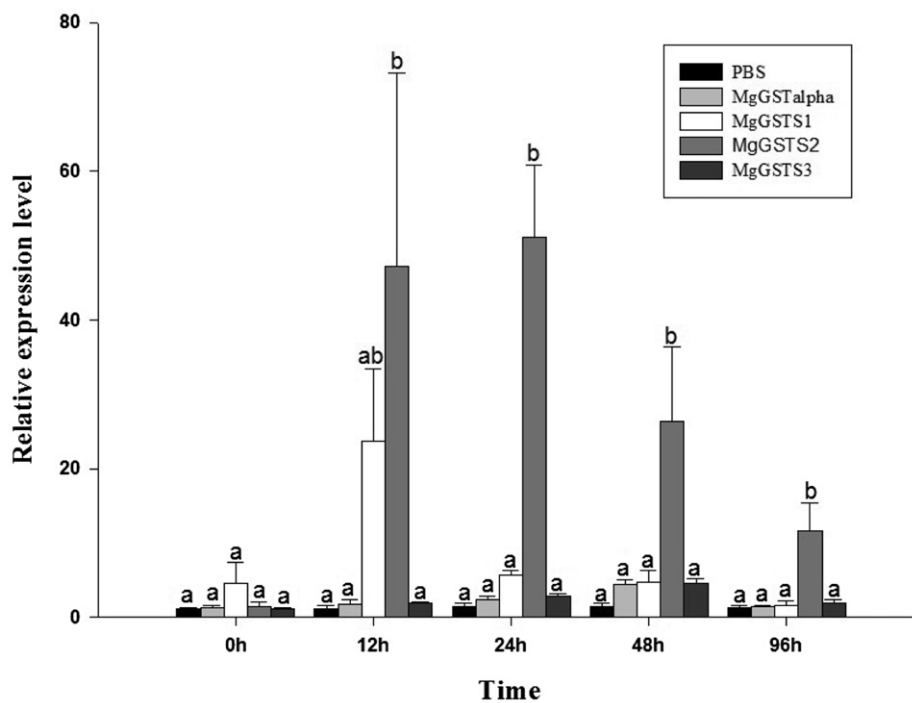


**Fig. 5.** Temporal expression profile of MgGST $\alpha$ , MgGSTS1, MgGSTS2, and MgGSTS3 mRNA in hemocytes after bacterial challenge measured by quantitative real-time PCR. The mRNA expression level is calculated relative to actin expression and shown as mean  $\pm$  S.E. ( $n = 4$ ). Data in the same exposure time with different letters are significantly different ( $P < 0.05$ ).

## Acknowledgments

The authors were grateful to all the laboratory members for continuous technical advice and helpful discussion. This research was supported by National Key Technology Support Program (2011BAD13B0903) and the K.C. Wong Magna Fund.

## References

- [1] Hu B, Deng L, Wen C, Yang X, Pei P, Xie Y, et al. Cloning, identification and functional characterization of a pi-class glutathione-S-transferase from the freshwater mussel *Cristaria plicata*. *Fish Shellfish Immunol* 2012;32:51–60.
- [2] Umasuthan N, Revathy KS, Lee Y, Whang I, Choi CY, Lee J. A novel molluscan sigma-like glutathione S-transferase from *Manila clam*, *Ruditapes philippinarum*: cloning, characterization and transcriptional profiling. *Comp Biochem Physiol C* 2012;155:539–50.
- [3] Mu C, Wang Q, Yuan Z, Zhang Z, Wang C. Identification of glutaredoxin 1 and glutaredoxin 2 gene from *Venerupis philippinarum* and their responses to benzo [a] pyrene and bacterial challenge. *Fish Shellfish Immunol* 2012;32:482–8.
- [4] Boutet I, Tanguy A, Moraga D. Characterisation and expression of four mRNA sequences encoding glutathione S-transferases pi, mu, omega and sigma classes in the Pacific oyster *Crassostrea gigas* exposed to hydrocarbons and pesticides. *Mar Biol* 2004;146:53–64.
- [5] Hayes JD, Flanagan JU, Jowsey IR. Glutathione transferases. *Annu Rev Pharmacol Toxicol* 2005;45:51–88.
- [6] Sheehan D, Meade G, Foley VM, Dowd CA. Structure, function and evolution of glutathione transferases: implications for classification of non-mammalian members of an ancient enzyme superfamily. *Biochem J* 2001;3:60–1.
- [7] Zhang L, Qiu L, Wu H, Liu X, You L, Pei D, et al. Expression profiles of seven glutathione S-transferase (GST) genes from *Venerupis philippinarum* exposed to heavy metals and benzo [a] pyrene. *Comp Biochem Physiol C* 2012;155: 517–27.
- [8] Canesi L, Barmo C, Fabbri R, Ciacci C, Vergani L, Roch P, et al. Effects of vibrio challenge on digestive gland biomarkers and antioxidant gene expression in *Mytilus galloprovincialis*. *Comp Biochem Physiol C* 2010;152:399–406.
- [9] Cellura C, Toubiana M, Parrinello N, Roch P. HSP70 gene expression in *Mytilus galloprovincialis* hemocytes is triggered by moderate heat shock and *Listonella anguillarum*, but not by *V. splendidus* or *Micrococcus lysodeikticus*. *Dev Comp Immunol* 2006;30:984–97.
- [10] Chen L, Mu C, Zhao J, Wang C. Molecular cloning and characterization of two isoforms of cyclophilin A gene from *Venerupis philippinarum*. *Fish Shellfish Immunol* 2011;31:1218–23.
- [11] Kumar S, Nei M, Dudley J, Tamura K. MEGA: a biologist-centric software for evolutionary analysis of DNA and protein sequences. *Brief Bioinform* 2008;9: 299–306.
- [12] Blanchette B, Feng X, Singh BR. Marine glutathione S-transferases. *Mar Bio Technol* 2007;9:513–42.
- [13] Chen J, Xiao S, Deng Y, Du X, Yu Z. Cloning of a novel glutathione S-transferase 3 (GST3) gene and expression analysis in pearl oyster, *Pinctada martensii*. *Fish Shellfish Immunol* 2011;31:823–30.
- [14] Ren HL, Xu DD, Gopalakrishnan S, Qiao K, Huang WB, Wang KJ. Gene cloning of a sigma class glutathione S-transferase from abalone (*Haliotis diversicolor*) and expression analysis upon bacterial challenge. *Dev Comp Immunol* 2009; 33:980–90.
- [15] Sinning I, Kleywegt GJ, Cowan SW, Reinemer P, Dirr HW, Huber R, et al. Structure determination and refinement of human alpha class glutathione transferase A1-1, and a comparison with the Mu and Pi class enzymes. *J Mol Biol* 1993;232:192–212.
- [16] Dirr HW, Wallace LA. Role of the C-terminal helix 9 in the stability and ligand in function of class  $\alpha$  glutathione transferase A1-1. *Biochemistry* 1999;38: 15631–40.
- [17] Ivarsson Y, Mackey AJ, Edalat M, Pearson WR, Mannervik B. Identification of residues in glutathione transferase capable of driving functional diversification in evolution. *J Biol Chem* 2003;278:8733–8.
- [18] Bugge DM, Hegaret H, Wikfors GH, Allam B. Oxidative burst in hard clam (*Mercenaria mercenaria*) haemocytes. *Fish Shellfish Immunol* 2007;23:188–96.
- [19] Segal A. How neutrophils kill microbes. *Annu Rev Immunol* 2005;23: 197–223.
- [20] Wan Q, Whang I, Lee J. Molecular cloning and characterization of three sigma glutathione S-transferases from disk abalone (*Haliotis discus discus*). *Comp Biochem Physiol B* 2008;151:257–67.
- [21] Contreras-Vergara CA, Harris-Valle C, Sotelo-Mundo RR, Yepiz-Plascencia G. A mu-class glutathione S-transferase from the marine shrimp *Litopenaeus vannamei*: molecular cloning and active-site structural modeling. *J Biochem Mol Tox* 2004;18:245–52.
- [22] Lee YM, Seo JS, Jung SO, Kim IC, Lee JS. Molecular cloning and characterization of theta-class glutathione S-transferase (GST-T) from the hermaphroditic fish *Rivulus marmoratus* and biochemical comparisons with alpha-class glutathione S-transferase (GST-A). *Biochem Biophys Res Commun* 2006;346:1053–61.
- [23] Liao WQ, Liang XF, Wang L, Lei LM, Han BP. Molecular cloning and characterization of alpha class glutathione S-transferase gene from the liver of silver carp, bighead carp, and other major Chinese freshwater fishes. *J Biochem Mol Toxicol* 2006;20:114–26.
- [24] Ren Q, Sun RR, Zhao XF, Wang JX. A selenium-dependent glutathione peroxidase (Se-GPx) and two glutathione S-transferases (GSTs) from Chinese shrimp (*Fenneropenaeus chinensis*). *Comp Biochem Physiol C* 2009;149:613–23.